

APPLIED ECOLOGY

Marine high temperature extremes amplify the impacts of climate change on fish and fisheries

William W. L. Cheung^{1*}, Thomas L. Frölicher^{2,3}, Vicky W. Y. Lam¹,
 Muhammed A. Oyinlola¹, Gabriel Reygondeau¹, U. Rashid Sumaila^{1,4,5}, Travis C. Tai¹,
 Lydia C. L. Teh¹, Colette C. C. Wabnitz^{1,6}

Extreme temperature events have occurred in all ocean basins in the past two decades with detrimental impacts on marine biodiversity, ecosystem functions, and services. However, global impacts of temperature extremes on fish stocks, fisheries, and dependent people have not been quantified. Using an integrated climate-biodiversity-fisheries-economic impact model, we project that, on average, when an annual high temperature extreme occurs in an exclusive economic zone, 77% of exploited fishes and invertebrates therein will decrease in biomass while maximum catch potential will drop by 6%, adding to the decadal-scale mean impacts under climate change. The net negative impacts of high temperature extremes on fish stocks are projected to cause losses in fisheries revenues and livelihoods in most maritime countries, creating shocks to fisheries social-ecological systems particularly in climate-vulnerable areas. Our study highlights the need for rapid adaptation responses to extreme temperatures in addition to carbon mitigation to support sustainable ocean development.

INTRODUCTION

Marine fisheries are an important part of the global food system, generating economic benefits (1, 2), providing critical nutrients (3), and supporting people's livelihoods (4). These benefits are particularly pertinent for coastal communities in developing countries and indigenous communities (5). Recent international assessments (6, 7) have highlighted the predominantly negative impacts of climate change on marine ecosystems and fisheries. Previous studies project a global decline in total animal biomass (8), potential fisheries catches (9), economic benefits (10), and employment (11) under climate change. However, these works focused exclusively on the impacts of decadal-scale mean climate change, with the additional effects of climate variabilities such as marine extreme temperature events remaining unexamined.

A number of studies have documented large episodic shocks to marine social-ecological systems as a result of marine temperature extremes. These extreme events occur when ocean temperature is exceptionally high or low relative to the climatological average temperature of the area and can last for days, months, or a few years (12). Globally, the frequency of marine extreme high-temperature events that last for days or months (i.e., marine heatwaves) has doubled since 1982 and is projected to increase further under continued global warming (12, 13). Periods of extreme high ocean temperature (14) are already affecting many ecosystems (15), causing species' range shifts (16, 17), reproductive failure and increased mortalities in marine species (18), mass coral reef bleaching (19), and die-offs of kelp forests (20) and other coastal biogenic habitats (21). These ecological responses to extreme temperature events are having rippling

effects onto human communities, as many depend on the marine environment as a source of food, income, and livelihood and as a way of life (22, 23). These impacts can weaken the adaptive capacity of the ecological, social, and resource management systems to climate change. Therefore, fisheries' climate impact assessments need to account for the ecological, economic, and social dimensions of extreme temperature events in the context of decadal-scale climate change. However, with the exception of a few studies at the local scale (24), little is known about the global impact of marine temperature extremes on fisheries and dependent human communities.

There are multiple ways to define and characterize marine temperature extremes, and the choice of definition depends on the study's objectives (25, 26). Here, we focus on annual high temperature extremes, defined as the annual sea surface temperature (SST) anomalies exceeding the 95th percentile of a shifting baseline from 1950 to 2100 (Materials and Methods). Under a shifting baseline, high temperature extremes emerge solely because of natural variability that adds to changes due to long-term mean ocean warming (Fig. 1). By using annual mean temperature data, we focus on temperature extremes that last at least 1 year, as these events often have the largest impacts on fisheries (Materials and Methods). Moreover, annual temperatures are used instead of shorter time frames because of the longer life cycle of most fish stocks considered here that generally integrate the impacts of temperature variations on populations across longer time frames. This study focuses largely on the impacts of high-temperature extreme events, as these impacts have been of broad concern for marine conservation and seafood production sectors. However, annual cold temperature perturbations may reverse the negative impacts from high temperature extremes. Therefore, we examine whether marine annual cold temperature extremes ("cold spells") would lead to impacts that are opposite to those of marine high-temperature extreme events.

We use an integrated climate-marine biodiversity-fisheries-economic impact model (27) to quantify the impact of marine high temperature extremes on global fisheries and dependent human communities. The modeling approach aims to provide a consistent framework that incorporates the current knowledge about marine

¹Institute for the Oceans and Fisheries, The University of British Columbia, Vancouver, British Columbia, Canada. ²Climate and Environmental Physics, Physics Institute, University of Bern, Bern, Switzerland. ³Oeschger Centre for Climate Change Research, University of Bern, Bern, Switzerland. ⁴School of Public Policy and Global Affairs, The University of British Columbia, Vancouver, British Columbia, Canada. ⁵Institute for Environment and Development (LESTARI), Universiti Kebangsaan Malaysia, Bangi, 43600 Selangor, Malaysia. ⁶Stanford Center for Ocean Solutions, Stanford University, Stanford, CA, USA.

*Corresponding author. Email: w.cheung@oceans.ubc.ca

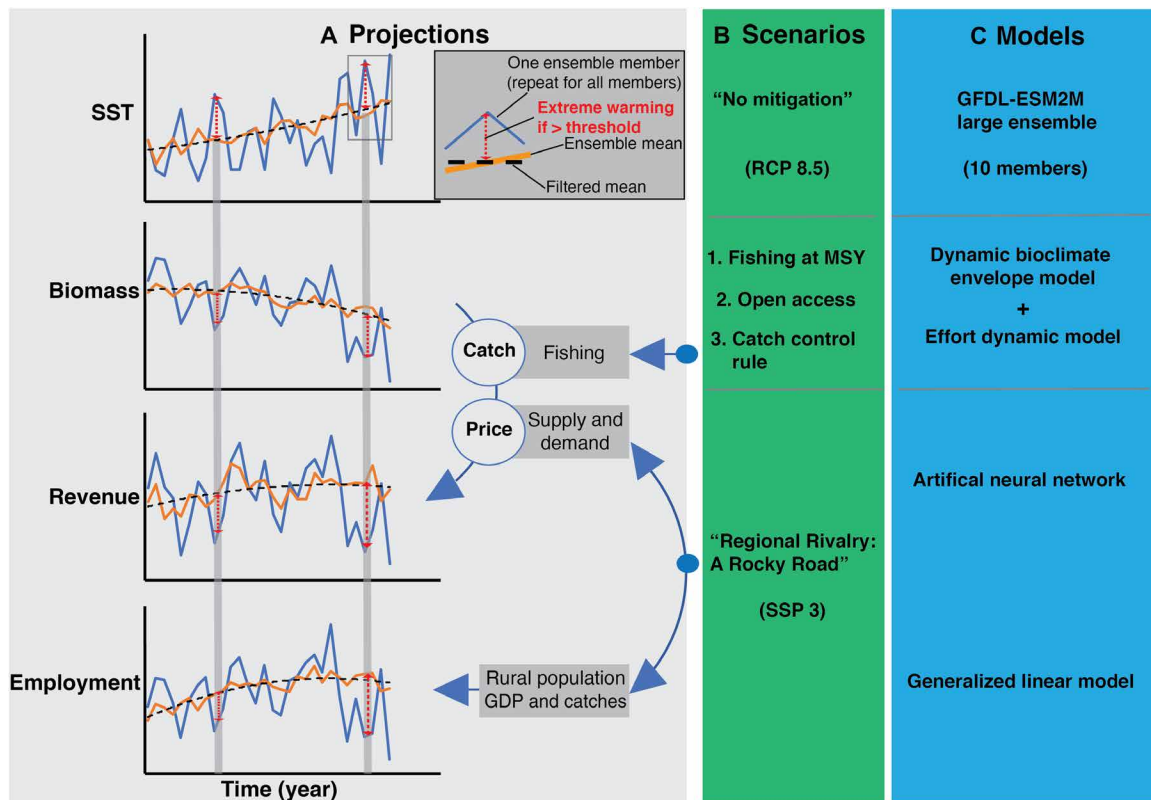


Fig. 1. Diagram illustrating this study's methodological framework. It includes three components: (A) projections, (B) scenarios, and (C) models. MSY, maximum sustainable yield (see Materials and Methods). GDP, gross domestic product; GFDL-ESM2M, Geophysical Fluid Dynamics Laboratory Earth System Model 2M.

fisheries social-ecological systems and applies it to project the systems' future under scenarios that integrate different climatic and socioeconomic drivers. We use the model outputs to calculate indicators of biological, fisheries, and socioeconomic impacts including biomass, catches, fisheries revenues, and fisheries-related employment (Materials and Methods). On the basis of the projected changes in these impact indicators, we highlight the potential risks of marine high temperature extremes on fish stocks and fisheries, thereby identifying the needs for appropriate response options.

Our modeling approach accounts for the linkages between climate, fisheries catches, fish prices, fishing effort, employment, and fisheries management under greenhouse gas emissions and socioeconomic scenarios (Representative Concentration Pathway or RCP8.5 for high greenhouse gas emission scenario and Shared Socioeconomic Pathway or SSP3, respectively; see Materials and Methods; Fig. 1) (27). We include 10,088 stocks of fishes and invertebrates [each stock is delineated by a species in an exclusive economic zone (EEZ)] that accounted for 41% of global fisheries catches in 2016 and 866 species from 265 countries' EEZs (i.e., excluding the high seas and considering Atlantic, Arctic, and Pacific Canada for instance as three distinct EEZs) (Materials and Methods; fig. S1 and table S1) (28). The performance and uncertainties of the climate, marine biodiversity, fisheries, and employment components of the integrated model in representing changes in ocean conditions, biogeography, potential fisheries catches, and related jobs have been examined independently in previous studies and here (table S2) (27, 29).

RESULTS AND DISCUSSION

On average, the period 1981 to 2100 experienced a total of 13 to 14 annual extreme high-temperature events, as defined herein, across all EEZs. During these high annual temperature events, we found the surface ocean in EEZs to be, on average, $0.72 \pm 0.31^\circ\text{C}$ (SD) warmer than decadal-mean conditions (fig. S2). In addition to these episodic high-temperature events, surface waters of EEZs are projected to warm by $1.23 \pm 0.33^\circ\text{C}$ by 2041–2060 relative to 1986–2005 under RCP8.5 (fig. S3 and table S2). The magnitude of sea bottom temperature anomalies in the EEZs during those extreme events is significantly and positively correlated with surface temperature anomalies ($P < 0.05$; see Materials and Methods).

Regionally, EEZs projected to experience the highest intensity of annual extreme warming events and decadal-scale mean sea surface warming (i.e., above global averages) are located in the Pacific Ocean, including the Indo-Pacific, Eastern Central Pacific, and Northeast Pacific regions (Fig. 2A). In contrast, EEZs in the North Atlantic Ocean and parts of the Southern Ocean are projected to experience strong extreme warming events but relatively low decadal-scale mean warming (30). In addition, the occurrences of extreme high-temperature events are related to interannual and decadal climate variabilities. The occurrence of extreme high-temperature events across many regions of the ocean is often associated with the dominant climate modes. The occurrence of extreme high-temperature events is especially elevated during El Niño years (31, 32) and conversely reduced during La Niña years.

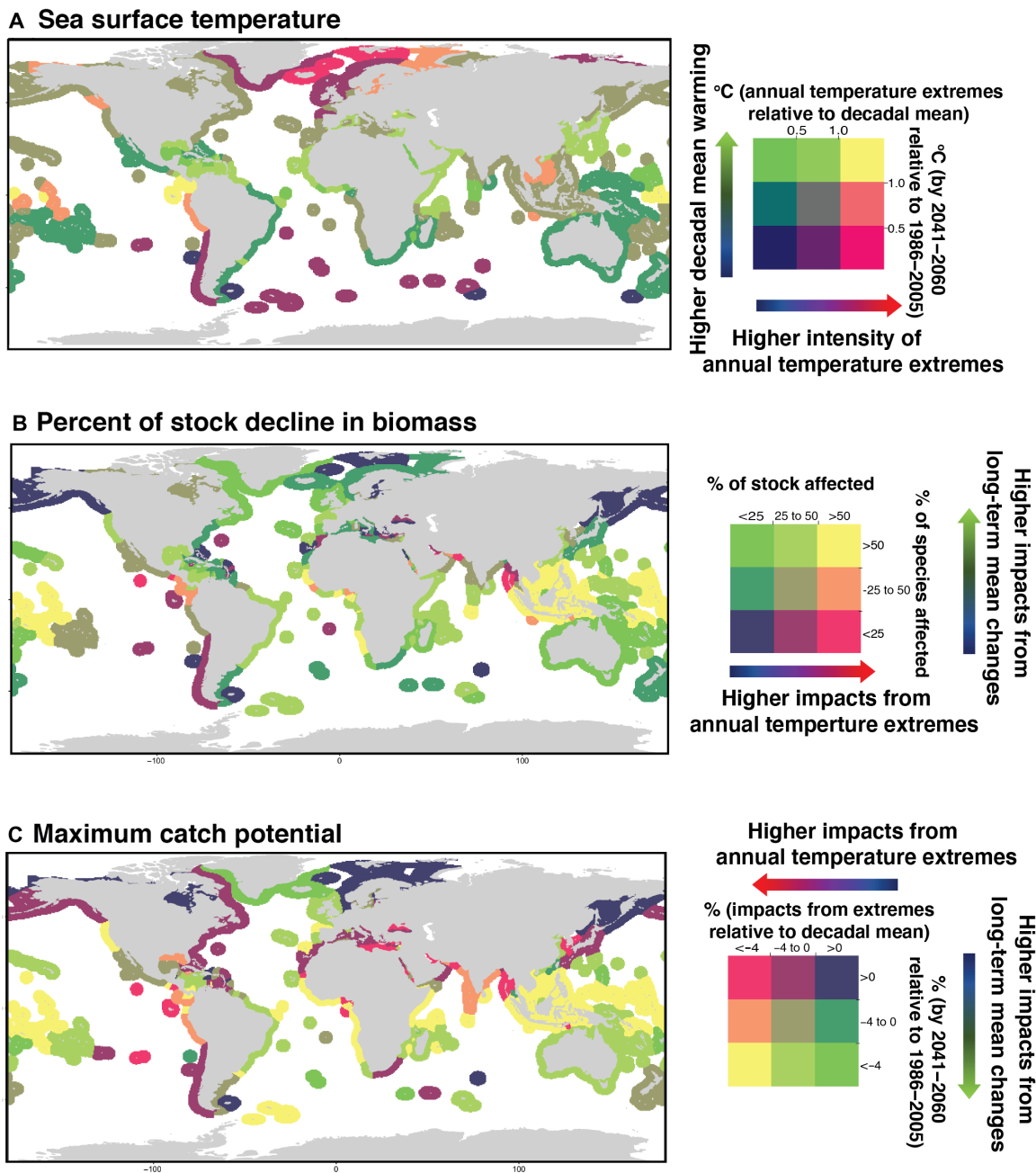


Fig. 2. Projected changes in the intensity of marine extreme high-temperature events and decadal-scale changes in mean sea surface warming and their impacts on stock biomass and their maximum catch potential by country's EEZs. (A) Increase in SST, **(B)** percent of stocks with biomass declines that are below a threshold of -3.6% , and **(C)** maximum catch potential. The threshold of -3.6% is the average rate of biomass decline per decade across all the studied stocks that is due to decadal-scale mean change by 2041–2060 relative to 1986–2005 under RCP8.5

Marine annual extreme high-temperature events add to decadal-mean warming impacts on fisheries stocks in the world's EEZs through declines in biomass (Fig. 2B). On average, during an extreme high-temperature event in an EEZ, 77% of the studied fish stocks are projected to decrease in biomass and 44% of them are projected to decline at magnitudes that are larger than the magnitude of the projected global decadal-scale mean decrease (-3.6% per decade) between 1986–2005 and 2041–2060 under RCP8.5 (Fig. 2B). Particularly, EEZs in the Indo-Pacific, South Pacific, and West Africa regions are

projected to register substantial declines in biomass due to both high temperature extremes and decadal-mean warming. Potential catches from EEZs that are projected to be positively affected by marine high temperature extremes are mainly in higher latitude regions, such as the North Atlantic and North Pacific Ocean.

Following changes in stock biomass, maximum catch potential is projected to decrease during annual high-temperature extreme events, in addition to impacts from decadal-scale mean climate change (Fig. 2C). The average rate of decline in maximum catch potential

among negatively affected stocks is projected to be 6% (ranging from less than 1 to 22%: 5th to 95th percentiles) relative to decadal-mean levels. Some stocks (21% of all studied stocks) are projected to increase by an average of 5% (<1 to 15%: 5th to 95th percentiles) in maximum catch potential during extreme high-temperature events. In comparison, decadal-scale mean warming leads to changes in maximum catch potential of stocks that range from a decrease of 11% to an increase of 8% per decade (5th and 95th percentiles, respectively) by 2050 relative to the recent past under RCP8.5. Thus, adding the impacts of annual high-temperature extremes to decadal-scale mean change is projected to result in an earlier emergence of risk of decrease in fish stocks and catches in the next few decades than from estimates based on mean changes alone. The earlier emergence of risk is consistent with observed impacts from extreme high-temperature events, for example, in the Northeast Pacific Ocean (e.g., the high-temperature extremes from 2013 to 2015) (24). In addition, over decadal time scales, accounting for the effects of annual low temperature extremes (“marine cold spells”) did not cancel out the impacts of marine high-temperature extremes due to asymmetries in biological sensitivities to ocean warming and cooling, such as thermal tolerance at species and community levels (see Supplementary Materials) (33). Empirical evidence from shifting stock ranges also suggests time lag in recovery of distribution from temperature perturbations in the Northwest Atlantic, resulting in complex changes in fish communities that are not linearly related to changes in temperature (34).

Variability in marine species’ thermal tolerance and associated biological responses to warming affect the spatial patterns of fisheries impacts from marine annual temperature extremes and decadal-scale mean change (Fig. 2, B and C). Tropical fisheries stocks are more sensitive to warming because of their narrower thermal tolerance range relative to temperate species (35), which is consistent with our biological model projections (9). Specifically, the tropical Pacific is projected to experience large impacts from decadal-scale mean change and to remain a hot spot for impacts from extreme high-temperature events on biomass and maximum catch potential. Catches from the tropical Pacific are dominated by tunas and billfishes, species known to be highly sensitive to climatic variabilities and change (36). Pelagic species are also exposed to larger temperature anomalies near the surface during extreme high-temperature events relative to demersal species that live closer to the sea bottom where the magnitude of high-temperature extremes is smaller than at the sea surface (Materials and Methods). In contrast, in the North Pacific and Atlantic, negative impacts from extreme high-temperature events and decadal-scale mean changes are, on average, smaller than for tropical regions. Exploited stocks in these temperate and sub-Arctic regions include relatively more demersal species than those in the tropical Pacific.

Our study suggests that marine annual extreme high-temperature events are likely to have negative impacts on dependent human communities across most EEZs (Fig. 3). We projected changes in fisheries revenues based on forecasted ex-vessel prices of targeted fisheries stocks from a machine learning algorithm and fisheries-related employment from an empirical model developed using global fisheries and socioeconomic databases (Materials and Methods). Fisheries-based revenue from selected stocks and fisheries-related employment in more than 80% of maritime countries in our study are projected to be affected negatively by extreme high-temperature events. We also find that more than 70% of the countries have

negative impacts on revenues that are larger than the average rate of decrease as a result of decadal-scale mean changes by mid-21st century relative to the recent past under RCP8.5. When extreme high-temperature events occur, revenues and employment are projected to decrease by a median of 3% (5th and 95th percentiles of 18 decrease to 2% increase) and 2% (13% decrease to 6% increase), respectively, relative to impacts under mean conditions (Fig. 3). These socioeconomic impacts of extreme high-temperature events are in addition to projected decreases in revenue and employment across most countries as a result of decadal-scale mean climate change. The projected impacts of marine annual high-temperature events on revenues are driven by changes in catch and price. Our model projects prices to increase with decreases in catch and increases in seafood demand under RCP8.5 and SSP3 (11), with a median increase in ex-vessel price of stocks of 120% (8 to 245%, interquartile range) by mid-21st century relative to the recent past. The projected impacts of temperature extremes on employment are driven by changes in catches and affected by scenarios of indirect drivers such as demography and economic development under SSP3. The extreme warming-related socioeconomic impacts are consistent with available, although limited, evidence from fisheries that have been affected by marine high-temperature extremes [e.g., Gulf of Alaska Pacific Cod (37), Northeast Atlantic lobster (38), and Tasmanian shellfish (39) fisheries].

The added impacts from marine high-temperature extremes to decadal-scale mean change would substantially increase the risk of impacts on countries that are strongly dependent on fisheries for income and livelihoods. For example, Ecuadorian fisheries are among those countries projected to be severely affected by both marine annual high-temperature extremes and decadal-scale mean climate change (Fig. 3, A and B), with a projected 10% reduction in revenue because of temperature extremes on top of a 25% decrease due to decadal-scale mean climate change by the mid-21st century relative to the recent past under RCP8.5. In Bangladesh, where fisheries-related sectors employ over one-third of the country’s labor force, an extreme high-temperature event is projected to result in an average loss of 2% of potential fisheries-related employment, equivalent to over 1 million jobs (4). This adds to a 12% fisheries employment decline projected for 2050 relative to the recent past as a result of decadal-scale mean climate change. Similarly, in Pacific Island states such as the Solomon Islands, marine high-temperature extremes are projected to exacerbate large projected reductions in fisheries revenue and employment caused by decadal-scale mean climate change (Fig. 3).

Using our integrated model that links the dynamic responses of fisheries stocks under climate change, with the economics of fishing and fishing effort (40), we examine the role of fisheries management actions in mitigating the effects of marine temperature extremes (Materials and Methods). Under two contrasting fishing scenarios (i.e., fishing under open access or managed through harvest control rules in response to changing stock biomass; see Materials and Methods), marine annual high-temperature extreme events are projected to continue to have negative impacts on marine stock biomass and catches relative to decadal-scale mean levels across most EEZs (Fig. 4). However, consistent with previous studies (41, 42), active fisheries management under decadal-scale mean climate change performs better in maintaining higher biomass relative to open access exploitation of stocks within EEZs (i.e., fishing is allowed to increase unabated). In addition, our results show that fisheries management through harvest control rules are projected to reduce the negative

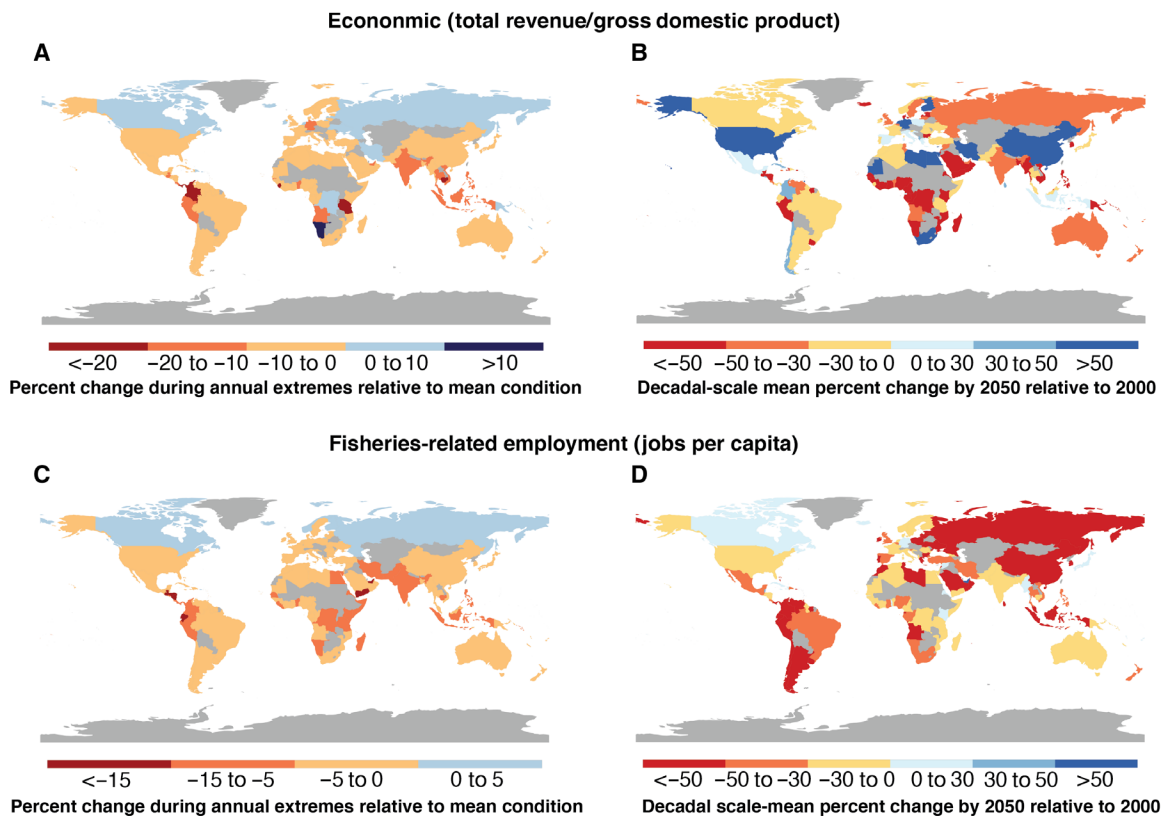


Fig. 3. Projected impacts of marine extreme high-temperature events and decadal-scale mean changes by 2041–2060 relative to 1986–2005, by fishing countries, under RCP8.5 and SSP3. (A) Projected average changes in fisheries revenue during an annual extreme high-temperature event. **(B)** Projected decadal-scale mean change in fisheries revenue per GDP. **(C)** Projected average changes in fisheries-related employment during an annual extreme high-temperature event. **(D)** Projected decadal-scale mean change in fisheries-related employment per capita. Grayed countries do not have a record of fishing on species included in this study.

impacts from high-temperature extremes relative to decadal-scale mean by 50% for biomass (from a cross-EEZ median of -7% under open access to -3% under harvest control rule) and 27% for catches (from a cross-EEZ median of -7 to -5%) (Fig. 4). The reduction in negative impacts on stock biomass is particularly large in EEZs that are projected to be hit hardest by marine high-temperature extremes, including those located in the Indo-Pacific (e.g., Gulf of Thailand, Indonesia, and Malaysia), Central America (e.g., Costa Rica, Peru, and Guatemala), Western Indian Ocean (e.g., Bangladesh), and West Africa (e.g., Ghana and Guinea). In contrast, for catches, some of the hardest affected EEZs are projected to become more sensitive to marine high-temperature events under the harvest control rule scenarios.

The harvest control rule scenario applied in this study adjusts allowable fishing levels based on predefined references of stock biomass. These fisheries management tactics make fishing levels more responsive to climate-driven changes in exploited stocks and specifically limit fishing if stock biomass decreases beyond the thresholds specified in the rules during extreme high-temperature events. Such a fishing control mechanism reduces the risk of stock depletion compared to the open access scenario where fishing is solely driven by economic factors. However, limiting fishing according to harvest control rules during marine extreme high-temperature events is projected to result in declines in catch because stock biomass drops below management thresholds during those extreme events. An example of such a decision includes the closure of the Gulf of Alaska Pacific cod fisheries because of the low stock biomass assessed in

relation to the marine extreme high-temperature event that affected large swaths of the Northeast Pacific in 2019–2020 (37).

The combination of high-temperature events and decadal-scale climate change may lead to long-term changes in fish stocks and fisheries that would be difficult to reverse (43). When simulating changes in fishing effort, a high-temperature extreme event's impacts on fish stocks and associated fisheries revenue affect active fishing effort and investment into changing fishing capacity in subsequent years. These effects influence the trajectory of stock biomass and catch and thus increase the variabilities in projected future biomass and catches. Moreover, the impacts of a high-temperature extreme are projected to affect fisheries development after the event, particularly for fisheries that are already close to biological or economic thresholds, e.g., stock biomass at a level close to the limit reference point of a harvest control rule when fishing would need to be substantially reduced or fisheries operating at bioeconomic equilibrium under open access (fisheries revenues equal cost). It would be useful for future studies to examine the reversibility or irreversibility of impacts of marine extreme high-temperature events on the social-ecological fisheries systems and implications for their resilience in supporting sustainable development.

The integrated climate-fisheries-socioeconomic model applied in this study facilitates the analysis of the linkages between social-ecological fisheries systems in responding to marine temperature extremes. However, the greater model complexity inevitably means that projections from the integrated model are likely to be more uncertain

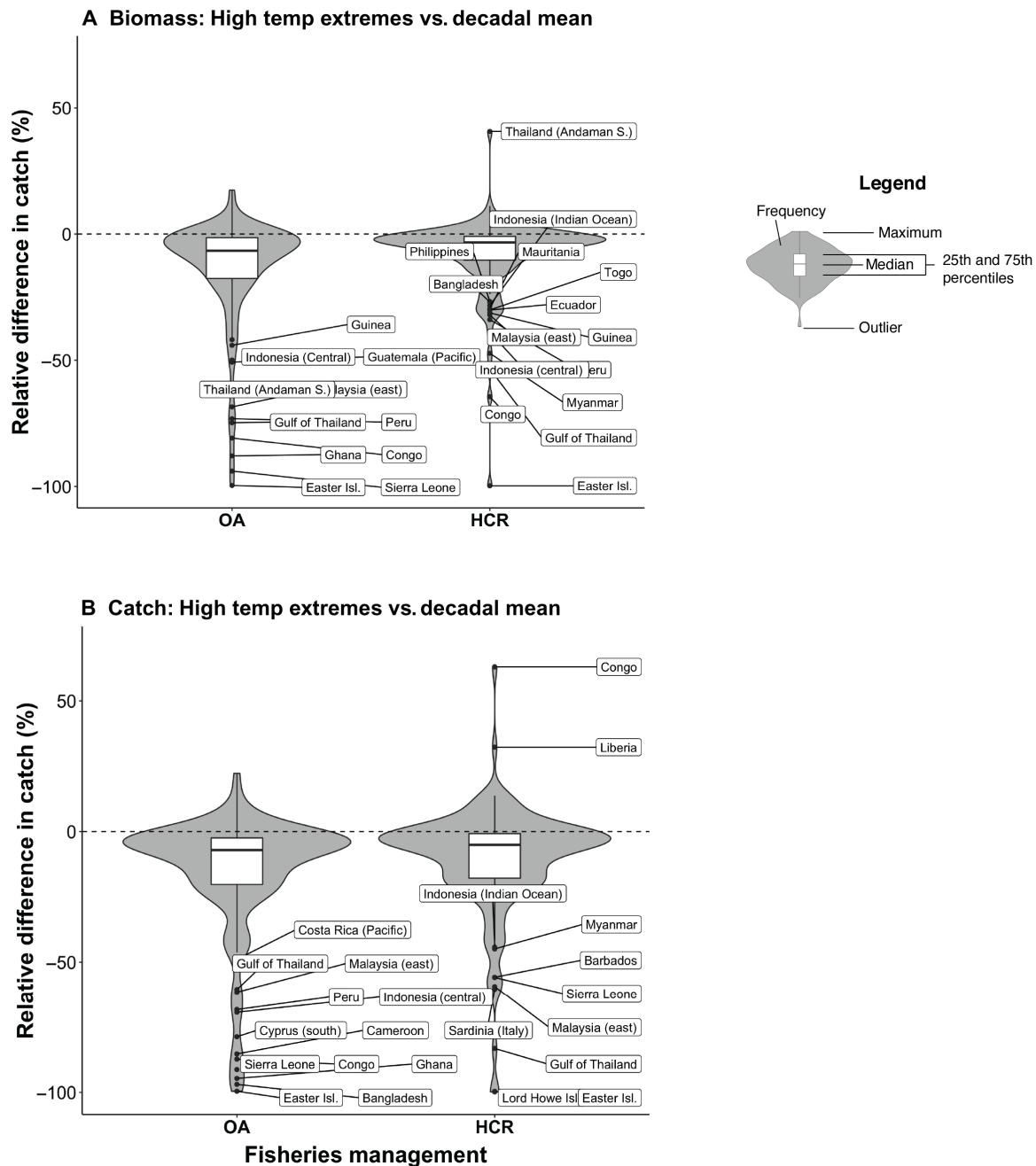


Fig. 4. Effects of marine extreme high-temperature events and fisheries management scenarios on biomass and fisheries catches. (A) Stock biomass under high-temperature extremes relative to decadal mean biomass. (B) Catches under high-temperature extremes relative to decadal mean catches. Both (A) and (B) include all the studied stocks in the EEZs for 2041–2060 under two fisheries management scenarios, SSP3 and RCP8.5. The two fisheries management scenarios considered are open access (OA) and harvest control rule (HCR) (Materials and Methods). The outliers represent data points beyond 1.5 times the interquartile range. The names of the respective EEZs to the outliers are displayed.

than from its components alone (table S2). While the main uncertainties and assumptions of each subcomponent of the integrated model have been discussed in previous studies (table S2) (11, 29, 44), some of these are particularly relevant to the exploration of the impacts of temperature extremes in this study. For the biophysical component, the main relevant assumptions and uncertainties include the coarse spatial resolution of the Earth system model simulations

used, the insufficient representation of processes that are driving some of the interannual variabilities of biological populations, and the effects and interactions of multiple human drivers on the exploited stocks that are not included in the model. For the human component, the model does not comprehensively capture the complex interactions between fisheries resources, fishing behaviors and fisheries management, the dynamic of fish prices, and

the interactions between different direct and indirect human drivers at different temporal and spatial scales.

While comprehensive characterization of the full range of uncertainties in projecting effects of temperature extremes on fisheries is beyond the scope of a single study, here, we examine the relative performance of our projections in representing plausible annual marine high-temperature extremes and their impacts on catches (see Materials and Methods). The ensemble simulations with the fully coupled GFDL-ESM2M (Geophysical Fluid Dynamics Laboratory Earth System Model 2M), by design, do not replicate the phasing of observed interannual climatic variability (44). However, the magnitude (median and maximum) of interannual variabilities of the simulated annual high-temperature extremes by EEZs is in relatively good agreement with observation-based estimates (fig. S10), if slightly overestimated. Nevertheless, the GFDL-ESM2M outperforms most other Coupled Model Intercomparison Project Phase 5 (CMIP5)-type models in simulating internal variability in SST over the historical period (45).

Since the biophysical and social-economic components of the integrated model are linked through catches, we compare the projected effects of annual high-temperature events on these stocks over the past six decades (1951–2016) with observational-based estimates (Materials and Method). The relationship between our projected maximum catch potential anomalies and observational-based catch anomalies under high-temperature extremes is much weaker than the comparison for temperature. The magnitude of the projected impacts on maximum catch potential from high-temperature extremes is smaller than those estimated from observational-based catch estimates. Thus, the projected changes can be considered more conservative. The biases and disagreement between model outputs and observational-based estimates are likely caused by both model and data uncertainties. Specifically, our model does not represent the full range of processes that are known to affect interannual variabilities of biological populations, such as the complex linkages between ocean biogeochemistry (beyond temperature) and stock-recruitment relationship, and their differences between stocks (46). In addition, given the global scope of this study, some of the model parameters, such as temperature preferences and demographic rates, are based on averages across populations and thus do not represent some of the population-specific characteristics that may affect the differences in interannual variabilities between stocks. Moreover, the uncertainties in simulation of ocean physical and biogeochemical conditions by the Earth system model (47), such as the insufficient representation of the dynamics of eastern boundary upwelling systems that support large historical catches (e.g., the Humboldt Current system that strongly influences Peruvian fisheries), also directly affect the biological projections driven by these simulations. There are also substantial uncertainties in the reporting and reconstruction of the observation-based catch data used in this study (48). The observational-based catches are affected by a large number of confounding factors such as the interannual variations in fishing activities and fisheries management driven by factors that are independent of stock abundance or distributions. For example, the collapse of the Peruvian anchoveta fisheries following the 1972 El Niño was likely the result of both low recruitment and decisions regarding catch quota by the management agency that yielded fishing levels exceeding the biological limits of the stocks (49). In addition, because of the constraint regarding the length of the observational-based time series, only two to three annual high-temperature extremes are identified per EEZ. The limited sample size of the observational-based estimations

exacerbates the uncertainties in the use of such data for comparison with model projections.

Regions where fisheries are projected to be most affected by high-temperature extremes include EEZs that are consistent with observational-based estimations (Fig. 5). Particularly, EEZs in our identified high-temperature extreme hot spots—including the Eastern Central Pacific (e.g., Ecuador and Costa Rica), West Africa (e.g., Senegal and Cape Verde), Indo-Pacific (e.g., Maldives, Philippines, and Vietnam), and around Central and South Pacific islands (e.g., Kiribati, Samoa, and U.S. Minor Outlying Islands)—have consistent and significant impacts estimated from both the observational-based estimations and our model projections ($P < 0.05$; Fig. 5 and fig. S11). For EEZs where agreement between model projections and observational-based catches estimates is weaker, the risk of impacts of high temperature extremes on fisheries is associated with lower confidence levels [e.g., the United Kingdom and Peru (Fig. 5)].

Our modeling framework offers a way to incorporate some of the current knowledge about marine fisheries social-ecological systems into analyses of the plausible effects of marine high-temperature extremes on stock biomass, catches, as well as revenue and employment opportunities generated by a diversity of fisheries. Hence, our findings provide a foundation for future research to build upon to gain better understanding of the effects of marine temperature extremes on marine fisheries social-ecological systems and inform approaches to support the sustainability of global fisheries. Such research should include the following: examining the effects of temperature extremes at higher temporal frequencies using daily or monthly climate model outputs, as well as the impacts of subsurface temperature extremes; exploring extreme events of other ecosystem drivers (25, 32) and their cumulative impacts, and the oceanographic, biological, and social-economic mechanisms underpinning the spatial and temporal variations of these impacts; examining the effects of temperature extremes on additional ecological and social-economic dynamics, such as trophic interactions and fisheries management; and evaluating a wider range of possible fisheries management and adaptation interventions to identify more effective measures to reduce risks and impacts on fisheries under climate change. Moreover, our findings show that marine cold spells (low-temperature extremes) could affect fisheries in ways other than the inverse of marine high-temperature extremes and that are presently poorly understood. Exploration of these phenomena and their impacts would represent a new and worthwhile research direction for studying marine temperature extremes. Additional development and testing of each model sub-components and the integrated analysis, such as through collation and comparison of model outputs with new observational datasets, could further increase the robustness of the findings and guide their further application. For example, this study uses a single algorithm to project the habitat suitability of exploited species, while previous studies suggested advantages in using multiple algorithms (29). Future studies could repeat the analyses presented here with multiple biological models or their components. Given the broad and multi-disciplinary scope of this study, we chose to focus our analysis on a high emission climate change scenario (RCP8.5) and a specific socioeconomic pathway, SSP3, associated with high challenges both in mitigation and adaptation. The RCP8.5 and SSP3 are at the extreme ends of the spectrum of climate change and social-economic scenarios. While the relationship between different levels of emissions and projected catches are strong (8, 9), the effects of other SSPs and their interactions with RCPs on fisheries have not been explored.

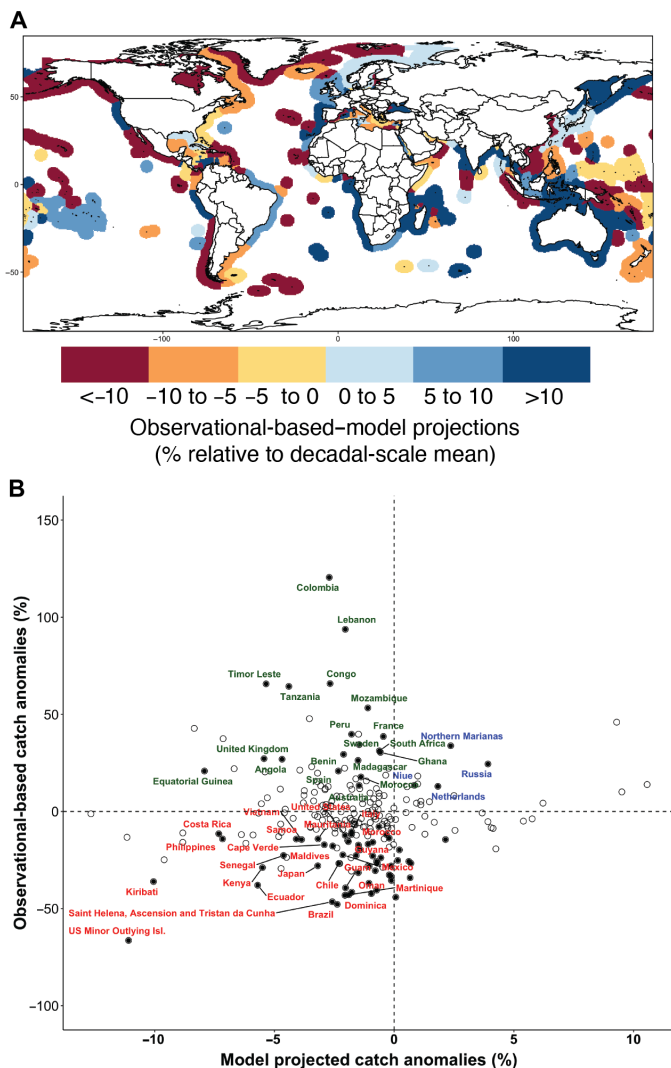


Fig. 5. Comparison between observational-based estimated effects of high-temperature extremes with model projections for the 1951–2016 period. (A) The differences between observational-based estimated changes in annual catches from EEZs relative to the mean conditions subtracted by those using maximum catch potential projected from the dynamic bioclimate envelope model (DBEM) driven by the Earth system model large ensemble simulations. (B) A comparison between annual catch anomalies relative to mean conditions under the identified high-temperature extremes using observational-based catches and projected maximum catch potential from the model by EEZs. The solid dots in (B) represent those EEZs with significant ($P < 0.05$) differences in catches under high-temperature events relative to the mean conditions (see Materials and Methods). Red and blue labels indicate EEZs with effects of high-temperature events estimated from observational-based and projected catches that are consistent in the direction of impacts (red, negative impacts; blue, positive impacts), while green labels indicate those that have inconsistent direction of impacts. Only the solid dotted EEZs are labeled.

Expanding the current simulations to alternative RCPs and SSPs may help elucidate the consequences of more effective greenhouse gas mitigation and alternative societal development pathways to reduce the risks and projected impacts of marine extreme high-temperature events on fish stocks and fisheries.

In summary, our study provides a unique global-scale analysis of the potential impacts of marine annual extreme high-temperature events on fish stocks, catches, fisheries revenues, and employment and the effects of fisheries management. We show that most biological and socioeconomic impacts from annual high temperature extremes are negative. Previous assessments of climate change impacts on marine fisheries have focused on mean change and thus largely underestimated climate risks, adding substantial challenge to human responses necessary for climate risk reduction. Particularly, this global analysis has identified potential hot spots of impacts where the biophysical and socioeconomic systems are at high risk to marine high-temperature events and decadal-scale mean warming. These hot spots include several EEZs in the Indo-Pacific, South Pacific, Central America, and West Africa regions. As some of these areas are underrepresented in existing studies of marine temperature extremes on fisheries and represent areas often highly dependent on a range of benefits derived from marine fisheries, our findings suggest that these regions could be priority areas for future impact and adaptation studies. Furthermore, while fisheries management can reduce impacts from long-term mean climate change, more climate-sensitive tactics may be more appropriate to help conserve fish stocks under marine extreme high-temperature events. In addition to climate-sensitive fisheries management, strategies are needed to help fishing sectors cope with the short-term socioeconomic impacts of lower catches or limited fishing as a result of high-temperature extremes. Our findings point to the need to mainstream consideration of extreme temperature events in standard climate-fisheries assessments, as well as the development of a more anticipatory and comprehensive set of solution options for securing a sustainable future for the ocean and dependent human communities.

MATERIALS AND METHODS

Overview of scenarios and modeling approaches

We use an integrated global climate, marine biodiversity, fisheries, and economic impact model called “DIVERSE” (50) to quantify the impact of marine annual temperature extremes on exploited fish and invertebrate stock biomass, catches, and fisheries-dependent revenue and employment. We use the outputs from a large ensemble simulation of the fully coupled Earth system model GFDL-ESM2M developed at the GFDL to project changes in ocean conditions and their variabilities over time under the RCP8.5 scenario (see the “Large ensemble Earth system model simulations” section). We use the dynamic bioclimate envelope model (DBEM) to simulate changes in distribution, abundance, and catches of exploited marine fishes and invertebrates (see the “Modeling fisheries stock biomass and maximum catch potential” section). We apply a machine learning algorithm to forecast ex-vessel prices of targeted fisheries stocks (see the “Modeling ex-vessel prices” section). The algorithm is based on projected catches and aquaculture production to represent fish supplies to the market. We also include other economic indicators such as gross domestic product (GDP) per capita, population, and seafood consumption per capita under SSP3 to represent seafood demand from the market (see the “SSP and fishing scenarios” section). We use generalized linear models to project fisheries-related employment based on catches and socioeconomic conditions of relevant countries (see the “Modeling fisheries-related employment” section). Use of these models and scenarios enables us to endogenize the dynamic feedback between changes in supply and demand.

We simulate the dynamics of fishing effort and fisheries management using a bioeconomic fishing effort dynamic model (see the “Modeling fishing effort dynamics” section). In addition, we also described the Sea Around Us catch data that are used in this study.

Large ensemble Earth system model simulations

The 10-member ensemble simulation was conducted with the fully coupled Earth system model 2M developed at the GFDL (GFDL-ESM2M) (51, 52). The ocean model MOM4p1 (50) has a nominal horizontal resolution of 1° latitude by 1° longitude, increasing toward the equator to ½°, and 50 vertical levels. The Tracers of Phytoplankton with Allometric Zooplankton version 2.0 is the ocean biogeochemistry and ecology model included in GFDL-ESM2M. The GFDL-ESM2M skillfully simulates the observed large-scale pattern of biogeochemical properties (47) and marine temperature extremes’ intensity (13) and captures the increase in marine high-temperature extreme days over the 1982–2016 satellite period (12).

The ensemble simulations were initialized through tiny perturbations to the initial climate state in 1950. The first ensemble member was branched into 9 additional members using 2 to 10 January 1950 of the first ensemble member for the initial conditions of members 2 to 10 (53). The ensemble members are independent realizations after about 3 years of simulation for surface waters and about 10 years at a depth of 300 m (54). The 10 ensemble members cover the historical 1950–2005 period and follow the RCP8.5 scenario over the 2006–2100 period. RCP8.5 is a high emission scenario without effective climate policies and projects a net radiative forcing of 8.5 W m⁻² by the end of the 21st century. In GFDL-ESM2M, atmospheric surface temperature in the RCP8.5 ensemble is projected to increase by 3.2°C between preindustrial times and 2081–2100.

Projecting marine annual temperature extremes

We identify the projected occurrence of marine annual extreme temperature events in the EEZs of the world ocean for each of the 10 ensemble member simulations of GFDL-ESM2M. We define marine annual extreme temperature events using annual average SST anomalies relative to the smoothed ensemble mean SST across the ensemble members (with a cubic spline filter, using the `smooth.spline` function in R to remove any residual interannual temperature variabilities of the ensemble mean SST), with marine annual high-temperature extreme events being identified to occur when SST is above the 95th percentile of the SST anomalies (24). Previous definitions of marine extreme temperature events (13, 31) often used fixed baselines (e.g., preindustrial conditions). Here, we use a shifting baseline (i.e., the ensemble mean) against which marine annual extreme temperature events are defined. This has allowed us to isolate the changes in marine annual extreme temperature event characteristics that arise because of changes in natural internal variability of the climatic system alone and to compare these changes with the decadal-mean changes that are driven by climate change (Fig. 1).

The “shifting baseline” definition of marine high temperature extremes is consistent with that used in (55). Jacox *et al.* (55) applied this definition to study the thermal displacement in the surface ocean, which is directly connected to our study, as our projections on distribution and abundance of fish stocks and their catches are partly driven by the thermal displacement of the ocean. The advantage of shifting the baseline in time is that one can more clearly partition to what extent marine extreme high-temperature events are related to a mean background warming or to changes in temperature variance,

which is particularly useful to elucidate the contributions of the effects of these variabilities on top of long-term mean changes. Other definitions of annual extreme temperature events have been used in the literature for other applications, e.g., (14, 15, 31, 56), and these definitions have been reviewed by studies such as that of Burger *et al.* (25) and Benthuisen *et al.* (17). The definition used here is particularly useful to elucidate the contributions of temperature variance in addition to long-term mean changes on fish stocks and fisheries.

For every marine annual extreme temperature event identified from each ensemble member, we characterize its intensity (SST anomalies relative to the smoothed ensemble mean values) and occurrence year. We then quantify the impacts of marine annual extreme temperature events on stock biomass, catches, as well as revenue and employment for fisheries-dependent communities. We compare the impacts due to marine extreme temperature events with decadal-scale mean changes over the 1981–2100 period.

Modeling fisheries stock biomass and maximum catch potential

We used the DBEM to simulate changes in distribution, abundance, and catches of exploited marine fishes and invertebrates. The structure of the DBEM is described in (29), and we summarize pertinent aspects of the model here, with details of the model described in the Supplementary Materials. First, the current distributions of commercially exploited species, representing the average pattern of relative abundance in recent decades (i.e., 1970–2000), were produced using a species distribution modeling algorithm described in (57). The model then calculated an index of habitat suitability for each species (P) in each spatial cell i from temperature (bottom and surface temperature for demersal and pelagic species, respectively), bathymetry, specific habitats (coral reef, continental shelf, slope, and seamounts), salinity (bottom and surface temperature for demersal and pelagic species, respectively), and sea ice with 30-year averages of outputs from 1971 to 2000 from GFDL-ESM2M. For anadromous species, our model represents the marine phase of their life cycle only. Next, DBEM estimated the temperature preference profile of each species by overlaying the estimated species distribution (29, 58) with annual seawater temperature and calculated the area-corrected distribution of relative abundance across temperature for each year from 1971 to 2000, subsequently averaging annual temperature preference profiles. Particular life stages at specific times of a year may be more sensitive to temperature. However, this study includes thousands of exploited fish stocks for which information about particularly sensitive time windows within a year are not available. Movement and dispersal of adults and larvae were modeled through advection-diffusion-reaction equations for larvae and adult stages using eq. S5 (A and B, respectively). Carrying capacity in each cell is assumed to be a function of the unfished biomass of the population, the habitat suitability, and net primary production in each cell. The global unfished biomass of the population is estimated on the basis of the average of the top 10 annual catches by weight of the modeled species in the world from 1950 to 2004 and their intrinsic population growth rate. We assumed that the average of the top 10 annual catches was roughly equal to the maximum sustainable yield of the species. The initial carrying capacity (θ) in each cell is calculated by prorating the unfished biomass to each cell based on the predicted habitat suitability. The model predicts changes in size and growth for each species according to changes in temperature, oxygen, and pH in the ocean relative to initial conditions. Adult natural mortality

rate was estimated from an empirical equation (59). Biomass (B) and catch (C) were then calculated from the population mean body weight and abundance. The model had a spin-up period of 100 years using the climatological average oceanographic conditions from 1971 to 2000, thereby allowing the population to reach equilibrium before it was perturbed with oceanographic changes. To calculate maximum catch potential and assuming logistic population growth, exploitation rate is set to be equal to natural mortality rate M to have maximum equilibrium surplus production.

Projecting impacts on fisheries catches

The projections of species turnover and changes in maximum potential catches are consistent with other modeling studies and empirical observations, providing support to the validity of using its outputs to assess climate risk to marine fisheries (table S2). The projected species turnover is a result of shifts in distributions of the modeled species driven by changes in temperature, oxygen level, net primary production, salinity, and other ocean conditions. Previous studies have already shown that range shifts projected by DBEM are generally consistent with alternative species distribution models and projections from different structures (with different algorithms predicting habitat suitability and incorporation of ecosystem size spectrum as additional constraints on habitat's carrying capacity) of DBEM and with observed range shifts, where data exist. In terms of projecting catches, DBEM is shown to reproduce current patterns of maximum catch potential across large marine ecosystems, and its projections are qualitatively similar to projections that are based on or have incorporated size-based trophodynamic interactions (29).

Uncertainties associated with biomass and maximum catch potential projections include the coarse resolution of Earth system model outputs particularly for representing the dynamics of shelf seas and coastal waters, the assumption of the absence of species' evolutionary responses to a changing climate, and insufficient consideration of the effects of trophodynamics. However, notwithstanding these uncertainties, the modeling approach provides generally robust projections regarding the direction and relative intensity of climate impacts at the global scale.

Modeling ex-vessel price

Ex-vessel fish prices for commercial fish species for the period 1950 to 2010 are based on the latest Fisheries Economics Research Unit and Sea Around Us global database as reported by Tai *et al.* (60). To project the prices reported by Tai *et al.* (60) into the future, we use an artificial neural network (ANN) to develop scenarios of the annual average ex-vessel price of the fish species covered by our analysis. We used the `elm.fit` function in the R package ("nnfor") that applies the ANN algorithm described by Kourentzes *et al.* (61). We train the ANN algorithm to project prices for each fisheries stock using time series ex-vessel fish price data, combined with the following independent variables: catches of a species within the EEZ, global catches of the species of the stock, GDP per capita, and gross seafood consumption of the sovereign state of the EEZ and global seafood consumption. These input variables represent seafood supply and demand (62–64). The test reveals that the ANN developed can predict historical ex-vessel price dynamics that match historical data well. We, therefore, apply the ANN to project future changes in price given projected catches from each ensemble member simulation using DBEM and projected GDP and population size under SSP3.

The global ex-vessel fish price database that we used for fisheries prices is the third updated version of its kind (62–64). Prices from this database are matched to catch estimates from the Sea Around Us catch database. The price estimation model follows a rule-based schematic to first match raw price data to catches and then estimates prices using a country-product dummy model when raw prices were not available for a given taxa-country-year combination (60, 65, 66). The ex-vessel price, p_{ijt} , in country i , taxa j , and year t can be estimated with

$$p_{ijt} = IP_{j,t} \cdot PPP_{i,t} \cdot u_{ijt} \quad (1)$$

where $IP_{j,t}$ is the international price of taxa j in year t , $PPP_{i,t}$ is the purchasing power parity for country i in year t , and u_{ijt} is the error term. Taking the natural logarithm of the equation, we obtain the dummy model

$$y_{ijt} = a_{j,t} + B_1 \cdot x_{1,t} + B_2 \cdot x_{2,t} + \dots + B_n \cdot x_{n,t} + \varepsilon_{ijt} \quad (2)$$

where y_{ijt} is the natural log of the reported price, $a_{j,t}$ is the natural log of the international price, and B is the dummy variable for the known coefficient $x_{n,t}$ equal to the natural log of the country effect on price. The number of countries (i.e., observations) is represented by n from $j = 1, 2, \dots, n$. The error term ε is normally distributed with mean 0 and constant variance σ^2 and related to u in eq. S1 such that $\varepsilon = \ln(u)$.

By rearranging Eq. 2 and solving for a , the model first relates ex-vessel prices (y) based on taxonomic classification and estimates a global "international" price using a country- and year-specific purchasing power parity (67). Matching ex-vessel prices follows a rule-based schematic based on taxonomic classification and ISSCAAP (International Standard Statistical Classification of Aquatic Animals and Plants) grouping, first matching at the species level and then broader categories (e.g., genus + ISSCAAP, genus, family + ISSCAAP, etc.). These international fish prices can then be converted to the currency for the country of interest and, thus, the ex-vessel price for a particular taxa j in country i .

Prices are converted to a common currency (U.S. dollars) and corrected for inflation using the U.S. consumer price index from the U.S. Bureau of Labor Statistics. Country-specific inflation is assumed to be captured by relative purchasing power parity between countries. One of the major assumptions of the price estimation model is that species are priced relatively similarly across countries (i.e., a global price) and that interannual variation in fish prices are represented in the purchasing power of the currency. Prices used in this analysis are the weighted average price across end product use (e.g., direct human consumption, fishmeal, and fish oil) (60).

We develop and use an ANN model to predict annual ex-vessel prices for each fisheries stock. We use the `elm.fit` function in the R package (nnfor) that applies the ANN algorithm described in (61). The prediction of ex-vessel prices includes four main steps (fig. S6).

In step 1, a set of historical time series data (1960 to 2010) are selected on the basis of economic theories that predict potential relationship of these variables with ex-vessel price by fisheries species. To represent domestic seafood production and supply, we include reported catches of the stock and mariculture production while domestic demand is represented by population size of the country, its GDP per capita, and seafood consumption per capita (62–64). A 5-year running median was then applied to each time series to smooth

large interannual price variation that may likely be due to factors exogenous to what we considered.

In step 2, for each fisheries stock, we apply the processed time series data to train an ANN to predict ex-vessel prices. The methodology sets a number of hidden nodes (300) and estimates the weight of each connection to project future prices. While the methodology identifies the main component of a time series variability, it also allows various autocorrelation processes within and between variables in projecting ex-vessel prices. We performed 100 to 200 possible parallel pathways (i.e., simulations) to predict prices. We subsequently excluded the outlying lower and upper 1 percentiles of the pathways and computed the median ensemble pathway.

In step 3, to evaluate the uncertainty of the forecast predicted by the ensemble pathways, we compare the predicted price with reported price data from 2011 to 2015 that were not included in the training set of the Extreme Learning Machine algorithm (ELM). The model is considered validated if the test predicted that model median forecasts are significantly correlated with the reported values ($P < 0.05$) and over a R^2 (coefficient of determination) of 80%; otherwise, the model is retrained by increasing the number of hidden nodes and simulation.

In step 4, we applied the developed ANN to forecast prices on the basis of projected catches by species and their global catches, projected GDP, and population size under SSP3. Since there is no published global projection of seafood consumption, we assume that changes in per capita seafood consumption are dependent on the countries' GDP. Thus, using per capita seafood consumption and GDP time series from all the countries, we develop a generalized linear model to project future per capita seafood consumption. The model obtained has a significantly positive relationship between per capita seafood consumption and GDP per capita ($P < 0.01$, $R^2 = 0.9$).

The uncertainties in projecting seafood price decades into the future are large. The algorithm presented here aims to provide a consistent framework to investigate the potential effects of direct and indirect drivers on seafood prices that are consistent with data. Future studies could further refine the ANN algorithm or apply other algorithms to examine the impacts of marine temperature extremes on prices.

Modeling fisheries-related employment

We apply an empirical model to predict fisheries-related employment based on the generalized linear model described in (68). This model predicts total fisheries-related employment of a country based on its rural population, economic development status, and total catch. The model is developed using the Fisheries Economics global dataset of fisheries-related employment (4).

Two versions of generalized linear models, which differ in how they include the interaction terms between GDP and catches, have been developed. We use both models and calculate the weighted [by the models' Akaike information criterion (AIC)] average outputs from them. The parameter values of the models are given in table S5. Because the employment data are only available for a particular time period (standardized for 2010), each country is used as a sample. Fisheries-related jobs, rural population size, and catch are log-transformed for use in the models. Each model run is a combination of the three variables, starting with the total set of variables. Particularly, we hypothesize that higher catches would result in more employment for fisheries-related sectors, with everything else being equal. In addition, since many fisheries-related jobs occur in rural coastal areas, we assume that a higher rural population would also be related to higher fisheries-related employment. Moreover, small-scale labor-intensive

fisheries may be more dominant in less economically developed countries, while fisheries in developed countries are dominated by more technology-intensive fisheries that would require less labor per unit of catch. Thus, countries with higher GDP per capita would have lower fisheries-related employment. There may be interactions between income class and catches in relation to marine-related employment. The structures of the models are

$$\text{Employment} = a \cdot \log(\text{ruralpopulation}) + b \cdot \log(Y) + \sum_{i=1}^4 d \cdot \text{factor}(\text{gdppc}_i) + \log(Y) \cdot \sum_{i=1}^4 \text{factor}(\text{gdppc}_i) + \epsilon. \quad (\text{model 1})$$

$$\text{Employment} = a \cdot \log(\text{ruralpopulation}) + b \cdot \log(Y) + \sum_{i=1}^4 d \cdot \text{factor}(\text{gdppc}_i) + \epsilon. \quad (\text{model 2})$$

where ruralpopulation is the rural population size of each country; Y denotes catches; gdppc is the GDP per capita; and a , b , d , and ϵ are coefficients and intercepts of the function, with Gaussian (log-link) error distribution function.

The model (model 1) with the lowest AIC predicts that the number of fisheries-related jobs is significantly related to rural population size, total fisheries catch, and the economic status of the country, with interactions between the latter two factors ($P < 0.05$, table S5 and fig. S7). Total fish catch is positively related to the number of fishers, indicating that future increases in fish catch are projected to drive additional fisheries jobs. However, for middle- and high-income countries, as indicated by their GDP per capita rankings, the sensitivity of the number of jobs to catches is lower than in lower-income and lower-middle-income countries. This supports the hypothesis that fisheries employment in developed countries is likely to be structured differently than those in less developed countries. Rural coastal population size is also positively related to fisheries jobs, suggesting that countries with larger rural populations are expected to have proportionally more people engaged in fisheries. For the competing model (model 2), the conclusion is qualitatively similar to model 1, except that the model omits the potential interaction between catches and countries' economic status. We use the ensemble of models 1 and 2 to project changes in fisheries-related employment weighted by the model's AIC.

Modeling fishing effort dynamics

We apply a fishing effort dynamic model (EDM) to simulate changes in fishing effort, fisheries catches, revenues and profits under scenarios of climate change, and fisheries management as described in (40). Parameter values of the effort dynamic model are estimated for each EEZ-ocean basin unit using available databases, empirical equations, and time series of fisheries catches data from 1950 to 2014. The model includes two main components: a biomass dynamic model and a fisheries economic model.

The biological component of the effort dynamic model is driven by outputs from the DBEM. The linkages between the DBEM and the fishing effort dynamic model are one way, with outputs from the earlier model feed into the effort dynamic model. Specifically, the biological component of the EDM is a biomass dynamic model that assumes logistic population growth. The biomass dynamic model is initialized with two parameters: the intrinsic population growth rate (r) and the carrying capacity (K) of the fisheries stock. The model is driven by two variables that relate to climate change effects on biological production and changes in fishing mortality rate for

each exploited stock. For each stock, annual relative change in biomass is calculated from outputs of the DBEM. The computed relative change in biomass is then applied to the biomass dynamic model to simulate the effect of changes in abundance and production as a result of climate change. Changes in catchability and fishing mortality are calculated from the active fishing effort that is an output from the fisheries economic component of the EDM.

The fisheries economic submodel assumes that fishers seek to maximize their profit according to the Gordon-Schaefer model (69). The model is based on four key parameters: the effort response to profit coefficient, reinvestment ratio, capital depreciation rate, and the catchability coefficient of the fishing fleet. Changes in fishing effort are also driven by annual profit that is dependent on the catch of exploited stocks, ex-vessel price of fish, fishing cost, and subsidies received. Parameter values of the effort dynamic model are estimated for each EEZ-ocean basin unit using available databases, empirical equations, and time series of fisheries catches data from 1950 to 2014. Some initial parameters for the fisheries economic model are estimated on the basis of published datasets, while others are estimated by fitting the model with catch data reported in the Sea Around Us catch database. Unit ex-vessel price of catch is from the Fisheries Economics Research Unit price database (60). Initial (first year) fishing cost is estimated on the basis of a cost per unit of total revenue that is calculated from the reported total fishing cost from (70) and the total revenue from (10). Subsidies, expressed as a proportion of the total fishing cost, are estimated on the basis of the global subsidy database (71, 72). Initial fishing effort is calculated from a catchability coefficient estimated by fitting the effort dynamic model with data. Other parameters that are estimated by model-data fitting include the rate of increase in catchability, the effort to profit response ratio, the effort exit/depreciation rate, the effort investment rate, the cost inflation rate, and the initial capital cost (expressed as a percentage of total revenue). A numerical optimization algorithm (using the R function `nlminb`) is used to search for the set of parameter values that minimize the sum-of-square error between the predicted total catch from the effort dynamic model and the reported catch from the Sea Around Us database. The full description of the model is documented in (40).

We examined the occurrence of “path dependence” in the projected responses of fisheries to marine annual extreme warming events driven by the natural internal variability of the climate system and the cascading effects on fisheries stocks and fisheries. This path dependence is visible in the increase in the anomalies of projected biomass and catches across ensemble members over time, as simulated by the fishing effort dynamic model even when anomalies of SST decrease slightly over time ($P < 0.05$; table S4).

SSP and fishing scenarios

The SSP scenario used in simulations here is SSP3, commonly referred to as “Regional Rivalry—A Rocky Road” (73). In this scenario, the world is characterized as fragmented by resurgent nationalism, rife with concerns about competitiveness and security, and dominated by regional conflicts, pushing countries to focus on mostly domestic issues (73). Slow economic development, poverty, and pervasive environmental degradation in some regions result in poor progress toward sustainability (74). It is used here, as it reflects a possible decision space based on recent policy choices by a number of leaders.

In accordance with the globally applicable SSPs (73), we assumed for economic growth and the world’s population to follow established

trends. The International Institute for Applied Systems Analysis (IIASA) and the National Center for Atmospheric Research have developed a set of population growth and urbanization projections. Under SSP3, relatively low investments in human capital and low income growth are thought to lead to relatively high fertility and population growth rates, despite high mortality rates, across the developing world. This leads to urban and rural settlement patterns across sub-Saharan Africa, the Middle East, India, and Southeast Asia that are very dense (75). In contrast, economic uncertainty leads to relatively low fertility rates and low population growth with rapidly aging populations in what are currently characterized as “low fertility” countries. Generally, however, migration is relatively limited, and urbanization proceeds slowly, partly because of poor urban planning that make cities unattractive destinations and slow socioeconomic development that limits mobility and employment opportunities in urban areas. Thus, at a global level, population growth rates are high while urbanization rates remain low, yielding a large rural population and concomitant low urban-to-rural population ratios (75). For GDP, three alternative interpretations of the SSPs by the teams from the Organization for Economic Co-operation and Development, the Potsdam Institute for Climate Impact Research, and the IIASA exist. Here, we followed GDP projections as developed by IIASA, which are based on harmonized assumptions for the interpretation of the SSP storylines in terms of the main drivers of economic growth (see IIASA supplementary note for further details: https://tntcat.iiasa.ac.at/SspDb/static/download/ssp_supplementary%20text.pdf).

We explore two fisheries management scenarios: (i) open access and (ii) implementation of harvest or catch control rules. For the “open access” scenario, we assume no management control on fishing effort and that exploitation of fisheries stocks within EEZs are considered open access. For the “harvest or catch control rule” scenario, we assume fisheries in the world’s EEZs to be managed according to a control rule dependent on the stock biomass level relative to the model baseline of 1950. Specifically, if biomass of a fisheries’ stock falls below 50% of the baseline, then fishing mortality is reduced by 50% of the preceding year’s level. If biomass declines further to 25%, then fishing mortality would be reduced by 75%, and if biomass is below 12.5% of the baseline, then fishing would be closed. This is reversed if stock biomass recovers. We run the fishing effort dynamic model with socioeconomic data (e.g., price, subsidies, and costs of fishing from 1950 to 2100; see the “Modeling fishing effort dynamics” section above), and these socioeconomic drivers are simulated under the SSP3 scenario.

Analyzing the impacts of marine annual extreme high-temperature events relative to decadal-scale mean change

We tested for the effects of occurrences of marine annual extreme high-temperature events on simulated biomass, maximum catch potential, revenue, potential fisheries-related employment, and “realized” catches using generalized linear models. Specifically, marine extreme high-temperature events estimated to occur in ensemble member simulation from 1981 to 2100 are treated as samples and are compared with the decadal-scale mean climate change effects in the same year. The generic statistical model is

$$\text{Impact} = a \cdot \text{factor}(\text{MHW}'_i) + b \cdot \text{factor}(\text{year}) + c \cdot \text{factor}(\text{others}) + d$$

where Impact represents the specific impact variables (e.g., biomass or employment) while MHW is the occurrence of marine extreme

high-temperature events in ensemble member i . We account for the effects, if any, of the temporal trends of impact indicators. We also included a factor “others” that refers to other additional dimensions whose effect on impact indicators (e.g., fisheries management) we test for. The coefficients for the terms are represented by a to c , while d is the intercept. For biomass and catches, as the distribution is skewed with a long tail of large values, we assume a log-link Gaussian distribution for the generalized linear model. For other impact variables, we assume a normal Gaussian distribution.

Sea around us catch data

We obtained catch data from the Sea Around Us reconstruction database (www.seararoundus.org). Specifically, we extracted annual catches (tonnes) by each EEZ and species from 1951 to 2016. Since the catch data provided by the Sea Around Us database used a wide variety of data sources and information to estimate different dimensions of “catch,” such as subsistence catch, recreational catch, and discards, which are missing from officially reported data (48), we used reconstructed catch in our analysis to capture a more comprehensive estimation of the total availability of nutrients from marine fisheries. The catch data are distributed onto 180,000, 30′ latitude by 30′ longitude spatial cells of the world ocean (76). The catch allocation process does not include climatic variables such as temperature that are used in projecting catch potential.

SUPPLEMENTARY MATERIALS

Supplementary material for this article is available at <https://science.org/doi/10.1126/sciadv.abh0895>

REFERENCES AND NOTES

- U. R. Sumaila, W. Cheung, A. Dyck, K. Gueye, L. Huang, V. Lam, D. Pauly, T. Srinivasan, W. Swartz, R. Watson, D. Zeller, Benefits of rebuilding global marine fisheries outweigh costs. *PLOS ONE* **7**, e40542 (2012).
- FAO, *The State of World Fisheries and Aquaculture 2018—Meeting the Sustainable Development Goals* (FAO, 2018).
- C. C. Hicks, P. J. Cohen, N. A. J. Graham, K. L. Nash, E. H. Allison, C. D’Lima, D. J. Mills, M. Roscher, S. H. Thilsted, A. L. Thorne-Lyman, M. A. MacNeil, Harnessing global fisheries to tackle micronutrient deficiencies. *Nature* **574**, 95–98 (2019).
- L. C. L. Teh, U. R. Sumaila, Contribution of marine fisheries to worldwide employment. *Fish Fish.* **14**, 77–88 (2013).
- A. M. Cisneros-Montemayor, D. Pauly, L. V. Weatherdon, Y. Ota, A global estimate of seafood consumption by coastal indigenous peoples. *PLOS ONE* **11**, e0166681 (2016).
- IPCC, *Summary for Policymakers. In: IPCC Special Report on the Ocean and Cryosphere in a Changing Climate* (IPCC, 2019).
- K. M. A. Chan, J. Agard, J. Liu, A. P. D. de Aguiar, D. Armenteras-Pascual, A. K. Boedihartono, William. W. L. Cheung, S. Hashimoto, G. C. H. Pedraza, T. Hickler, J. Jetzkowitz, M. Kok, M. Murray-Hudson, P. O’Farrell, T. Satterfield, A. K. Salsel, R. Seppelt, B. Strassburg, D. Xue, *IPBES Global Assessment on Biodiversity and Ecosystem Services* (Intergovernmental Science-Policy Platform on Biodiversity and Ecosystem Services, 2019).
- H. K. Lotze, D. P. Tittensor, A. Bryndum-Buchholz, T. D. Eddy, W. W. L. Cheung, E. D. Galbraith, M. Barange, N. Barrier, D. Bianchi, J. L. Blanchard, L. Bopp, M. Büchner, C. M. Bulman, D. A. Carozza, V. Christensen, M. Coll, J. P. Dunne, E. A. Fulton, S. Jennings, M. C. Jones, S. Mackinson, O. Maury, S. Niiranen, R. Oliveros-Ramos, T. Roy, J. A. Fernandes, J. Schewe, Y.-J. Shin, T. A. M. Silva, J. Steenbeek, C. A. Stock, P. Verley, O. L. Chen, S. S. Gulati, B. Worm, Global ensemble projections reveal trophic amplification of ocean biomass declines with climate change. *Proc. Natl. Acad. Sci.* **116**, 12907–12912 (2019).
- W. W. L. Cheung, G. Reygondeau, T. L. Frölicher, Large benefits to marine fisheries of meeting the 1.5 C global warming target. *Science* **354**, 1591–1594 (2016).
- V. W. Y. Lam, W. W. L. Cheung, G. Reygondeau, U. R. Sumaila, Projected change in global fisheries revenues under climate change. *Sci. Rep.* **6**, 32607 (2016).
- U. R. Sumaila, T. C. Tai, V. W. Y. Lam, W. W. L. Cheung, M. Bailey, A. M. Cisneros-Montemayor, O. L. Chen, S. S. Gulati, Benefits of the Paris Agreement to ocean life, economics, and people. *Sci. Adv.* **5**, eaau3855 (2019).
- C. Laufkötter, T. L. Frölicher, J. Zscheischler, High-impact marine heatwaves attributable to human-induced global warming. *Science* **369**, 1621–1625 (2020).
- T. L. Frölicher, E. M. Fischer, N. Gruber, Marine heatwaves under global warming. *Nature* **560**, 360–364 (2018).
- A. J. Hobday, L. V. Alexander, S. E. Perkins, D. A. Smale, S. C. Straub, E. C. J. Oliver, J. A. Benthhuysen, M. T. Burrows, M. G. Donat, M. Feng, N. J. Holbrook, P. J. Moore, H. A. Scannell, A. S. Gupta, T. Wernberg, A hierarchical approach to defining marine heatwaves. *Prog. Oceanogr.* **141**, 227–238 (2016).
- T. L. Frölicher, C. Laufkötter, Emerging risks from marine heat waves. *Nat. Commun.* **9**, 650 (2018).
- L. M. Cavole, A. M. Demko, R. E. Diner, A. Giddings, I. Koester, C. M. L. S. Pagniello, M. L. Paulsen, A. Ramirez-Valdez, S. M. Schwenck, N. K. Yen, M. E. Zill, P. J. S. Franks, Biological impacts of the 2013–2015 warm-water anomaly in the northeast Pacific: Winners, losers, and the future. *Oceanography* **29**, 273–285 (2016).
- J. A. Benthhuysen, E. C. J. Oliver, K. Chen, T. Wernberg, Editorial: Advances in understanding marine heatwaves and their impacts. *Front. Mar. Sci.* **7**, 147 (2020).
- J. F. Piatt, J. K. Parrish, H. M. Renner, S. K. Schoen, T. T. Jones, M. L. Arimitsu, K. J. Kuletz, B. Bodenstein, M. Garcia-Reyes, R. S. Duerr, R. M. Corcoran, R. S. A. Kaler, G. J. McChesney, R. T. Golightly, H. A. Coletti, R. M. Suryan, H. K. Burgess, J. Lindsey, K. Lindquist, P. M. Warzybok, J. Jahncke, J. Roletto, W. J. Sydeman, Extreme mortality and reproductive failure of common murrelets resulting from the northeast Pacific marine heatwave of 2014–2016. *PLOS ONE* **15**, e0226087 (2020).
- T. P. Hughes, J. T. Kerry, M. Álvarez-Noriega, J. G. Álvarez-Romero, K. D. Anderson, A. H. Baird, R. C. Babcock, M. Beger, D. R. Bellwood, R. Berkelmans, T. C. Bridge, I. R. Butler, M. Byrne, N. E. Cantin, S. Comeau, S. R. Connolly, G. S. Cumming, S. J. Dalton, G. Diaz-Pulido, C. M. Eakin, W. F. Figueira, J. P. Gilmour, H. B. Harrison, S. F. Heron, A. S. Hoey, J.-P. A. Hobbs, M. O. Hoogenboom, E. V. Kennedy, C.-y. Kuo, J. M. Lough, R. J. Lowe, G. Liu, M. T. McCulloch, H. A. Malcolm, M. J. McWilliam, J. M. Pandolfi, R. J. Pears, M. S. Pratchett, V. Schoepf, T. Simpson, W. J. Skirving, B. Sommer, G. Torda, D. R. Wachenfeld, B. L. Willis, S. K. Wilson, Global warming and recurrent mass bleaching of corals. *Nature* **543**, 373–377 (2017).
- T. Wernberg, D. A. Smale, F. Tuya, M. S. Thomsen, T. J. Langlois, T. De Bettignies, S. Bennett, C. S. Rousseaux, An extreme climatic event alters marine ecosystem structure in a global biodiversity hotspot. *Nat. Clim. Chang.* **3**, 78–82 (2013).
- N. L. Bindoff, W. W. L. Cheung, J. G. Kairo, J. Aristegui, V. A. Guinder, R. Hallberg, N. Hilmi, N. Jiao, M. saiful Karim, L. Levin, S. O’Donoghue, S. R. Purca Cuicapusa, B. Rinkevich, T. Suga, A. Tagliabue, P. Williamson, “Changing ocean, marine ecosystems, and dependent communities, in *Special Report on the Ocean and Cryosphere in a Changing Climate* (IPCC, 2019).
- D. A. Smale, T. Wernberg, E. C. J. Oliver, M. Thomsen, B. P. Harvey, S. C. Straub, M. T. Burrows, L. V. Alexander, J. A. Benthhuysen, M. G. Donat, M. Feng, A. J. Hobday, N. J. Holbrook, S. E. Perkins-Kirkpatrick, H. A. Scannell, A. S. Gupta, B. L. Payne, P. J. Moore, Marine heatwaves threaten global biodiversity and the provision of ecosystem services. *Nat. Clim. Chang.* **9**, 306–312 (2019).
- N. M. Wade, T. D. Clark, B. T. Maynard, S. Atherton, R. J. Wilkinson, R. P. Smullen, R. S. Taylor, Effects of an unprecedented summer heatwave on the growth performance, flesh colour and plasma biochemistry of marine cage-farmed Atlantic salmon (*Salmo salar*). *J. Therm. Biol.* **80**, 64–74 (2019).
- W. W. L. Cheung, T. L. Frölicher, Marine heatwaves exacerbate climate change impacts for fisheries in the northeast Pacific. *Sci. Rep.* **10**, 6678 (2020).
- F. A. Burger, T. L. Frölicher, J. G. John, Increase in ocean acidity variability and extremes under increasing atmospheric CO₂. *Biogeosciences* **17**, 4633–4662 (2020).
- E. C. J. Oliver, J. A. Benthhuysen, S. Darmaraki, M. G. Donat, A. J. Hobday, N. J. Holbrook, R. W. Schlegel, A. Sen Gupta, Marine heatwaves. *Annu. Rev. Mar. Sci.* **13**, 313–342 (2021).
- W. W. L. Cheung, M. A. Oyinlola, Dynamic integrated marine climate, biodiversity, fisheries, aquaculture and seafood market model (DIVERSE), in *Fisheries Centre Research Report* (Institute for the Oceans and Fisheries, The University of British Columbia, 2019), vol. 27.
- D. Pauly, D. Zeller, M. D. Palomares, *Sea Around Us Concepts, Design and Data* (2020); www.seararoundus.org.
- W. W. L. Cheung, M. C. Jones, G. Reygondeau, C. A. Stock, V. W. Y. Lam, T. L. Frölicher, Structural uncertainty in projecting global fisheries catches under climate change. *Ecol. Model.* **325**, 57–66 (2016).
- J. Marshall, K. Speer, Closure of the meridional overturning circulation through Southern Ocean upwelling. *Nat. Geosci.* **5**, 171–180 (2012).
- E. C. J. Oliver, M. G. Donat, M. T. Burrows, P. J. Moore, D. A. Smale, L. V. Alexander, J. A. Benthhuysen, M. Feng, A. S. Gupta, A. J. Hobday, N. J. Holbrook, S. E. Perkins-Kirkpatrick, H. A. Scannell, S. C. Straub, T. Wernberg, Longer and more frequent marine heatwaves over the past century. *Nat. Commun.* **9**, 1324 (2018).
- N. Le Grix, J. Zscheischler, C. Laufkötter, C. S. Rousseaux, T. L. Frölicher, Compound high-temperature and low-chlorophyll extremes in the ocean over the satellite period. *Biogeosciences* **18**, 2119–2137 (2021).

33. M. B. Araújo, F. Ferri-Yañez, F. Bozinovic, P. A. Marquet, F. Valladares, S. L. Chown, Heat freezes niche evolution. *Ecol. Lett.* **16**, 1206–1219 (2013).
34. M. D. Robertson, J. Gao, P. M. Regular, M. J. Morgan, F. Zhang, Lagged recovery of fish spatial distributions following a cold-water perturbation. *Sci. Rep.* **11**, 9513 (2021).
35. J. M. Sunday, A. E. Bates, N. K. Dulvy, Thermal tolerance and the global redistribution of animals. *Nat. Clim. Chang.* **2**, 686–690 (2012).
36. M. Lima, D. E. Naya, Large-scale climatic variability affects the dynamics of tropical skipjack tuna in the Western Pacific Ocean. *Ecography* **34**, 597–605 (2011).
37. W. Cornwall, Ocean heat waves like the Pacific's deadly "Blob" could become the new normal. *Science* (2019).
38. K. E. Mills, A. J. Pershing, C. J. Brown, Y. Chen, F.-S. Chiang, D. S. Holland, S. Lehuta, J. A. Nye, J. C. Sun, A. C. Thomas, R. A. Wahle, Fisheries management in a changing climate: Lessons from the 2012 ocean heat wave in the Northwest Atlantic. *Oceanography* **26**, 191–195 (2013).
39. E. C. J. Oliver, J. A. Benthuisen, N. L. Bindoff, A. J. Hobday, N. J. Holbrook, C. N. Mundy, S. E. Perkins-Kirkpatrick, The unprecedented 2015/16 Tasman Sea marine heatwave. *Nat. Commun.* **8**, 16101 (2017).
40. V. W. Y. Lam, A. Cineros-Montemayor, W. W. L. Cheung, in *Dynamic Integrated Marine Climate, Biodiversity, Fisheries, Aquaculture and Seafood Market Model (DIVERSE)*, W. W. L. Cheung, M. A. Oyinlola, Eds. (Institute for the Oceans and Fisheries, The University of British Columbia, 2019).
41. S. D. Gaines, C. Costello, B. Owashi, T. Mangin, J. Bone, J. G. Molinos, M. Burden, H. Dennis, B. S. Halpern, C. V. Kappel, K. M. Kleisner, D. Ovando, Improved fisheries management could offset many negative effects of climate change. *Sci. Adv.* **4**, eaao1378 (2018).
42. C. M. Free, T. Mangin, J. G. Molinos, E. Ojea, M. Burden, C. Costello, S. D. Gaines, Realistic fisheries management reforms could mitigate the impacts of climate change in most countries. *PLOS ONE* **15**, e0224347 (2020).
43. R. M. Suryan, M. L. Arimitsu, H. A. Coletti, R. R. Hopcroft, M. R. Lindeberg, S. J. Barbeaux, S. D. Batten, W. J. Burt, M. A. Bishop, J. L. Bodkin, R. Brenner, R. W. Campbell, D. A. Cushing, S. L. Danielson, M. W. Dorn, B. Drummond, D. Esler, T. Gelatt, D. H. Hanselman, S. A. Hatch, S. Haught, K. Holderied, K. Iken, D. B. Irons, A. B. Kettle, D. G. Kimmel, B. Konar, K. J. Kuletz, B. J. Laurel, J. M. Maniscalco, C. Matkin, C. A. E. McKinstry, D. H. Monson, J. R. Moran, D. Olsen, W. A. Palsson, W. S. Pegau, J. F. Piatt, L. A. Rogers, N. A. Rojek, A. Schaefer, I. B. Spies, J. M. Straley, S. L. Strom, K. L. Sweeney, M. Szymkowiak, B. P. Weitzman, E. M. Yasumiishi, S. G. Zador, Ecosystem response persists after a prolonged marine heatwave. *Sci. Rep.* **11**, 6235 (2021).
44. C. A. Stock, M. A. Alexander, N. A. Bond, K. M. Brander, W. W. L. Cheung, E. N. Curchitser, T. L. Delworth, J. P. Dunne, S. M. Griffies, M. A. Haltuch, J. A. Hare, A. B. Hollowed, P. Lehodey, S. A. Levin, J. S. Link, K. A. Rose, R. R. Rykaczewski, J. L. Sarmiento, R. J. Stouffer, F. B. Schwing, G. A. Vecchi, F. E. Werner, On the use of IPCC-class models to assess the impact of climate on Living Marine Resources. *Prog. Oceanogr.* **88**, 1–27 (2011).
45. L. Suarez-Gutierrez, S. Milinski, N. Maher, Exploiting large ensembles for a better yet simpler climate model evaluation. *Clim. Dyn.* (2021).
46. E. D. Houde, in *Fish Reproductive Biology* (John Wiley & Sons, 2016), pp. 98–187.
47. L. Bopp, L. Resplandy, J. C. Orr, S. C. Doney, J. P. Dunne, M. Gehlen, P. Halloran, C. Heinze, T. Ilyina, R. Séférian, J. Tjiputra, M. Vichi, Multiple stressors of ocean ecosystems in the 21st century: Projections with CMIP5 models. *Biogeosciences* **10**, 6225–6245 (2013).
48. D. Pauly, D. Zeller, Catch reconstructions reveal that global marine fisheries catches are higher than reported and declining. *Nat. Commun.* **7**, 10244 (2016).
49. L. W. Botsford, J. C. Castilla, C. H. Peterson, The management of fisheries and marine ecosystems. *Science* **277**, 509–515 (1997).
50. S. M. Griffies, Elements of the modular ocean model (MOM). *GFDL Ocean Group Tech. Rep.* **7**, 47 (2012).
51. T. L. Frölicher, K. B. Rodgers, C. A. Stock, W. W. L. Cheung, Sources of uncertainties in 21st century projections of potential ocean ecosystem stressors. *Glob. Biogeochem. Cycles* **30**, 1224–1243 (2016).
52. K. E. Taylor, R. J. Stouffer, G. A. Meehl, An overview of CMIP5 and the experiment design. *Bull. Am. Meteorol. Soc.* **93**, 485–498 (2012).
53. K. B. Rodgers, J. Lin, T. L. Frölicher, Emergence of multiple ocean ecosystem drivers in a large ensemble suite with an earth system model. *Biogeosciences* **11**, 18189–18227 (2015).
54. T. L. Frölicher, L. Ramseyer, C. C. Raible, K. B. Rodgers, J. Dunne, Potential predictability of marine ecosystem drivers. *Biogeosciences* **17**, 2061–2083 (2020).
55. M. G. Jacox, M. A. Alexander, S. J. Bograd, J. D. Scott, Thermal displacement by marine heatwaves. *Nature* **584**, 82–86 (2020).
56. E. C. J. Oliver, Mean warming not variability drives marine heatwave trends. *Clim. Dyn.* **53**, 1653–1659 (2019).
57. W. W. L. Cheung, V. W. Y. Lam, D. Pauly, in *Modelling Present and Climate-shifted Distributions of Marine Fishes and Invertebrates*, W. W. L. Cheung, V. W. Y. Lam, D. Pauly, Eds. (The University of British Columbia, 2008), vol. 16, pp. 5–50.
58. W. W. L. Cheung, R. Watson, D. Pauly, Signature of ocean warming in global fisheries catch. *Nature* **497**, 365–368 (2013).
59. D. Pauly, On the interrelationships between natural mortality, growth parameters, and mean environmental temperature in 175 fish stocks. *J. Cons. Int. Explor. Mer* **39**, 175–192 (1980).
60. T. C. Tai, T. Cashion, V. W. Y. Lam, W. Swartz, U. R. Sumaila, Ex-vessel fish price database: Disaggregating prices for low-priced species from reduction fisheries. *Front. Mar. Sci.* **4**, 363 (2017).
61. N. Kourentzes, D. K. Barrow, S. F. Crone, Neural network ensemble operators for time series forecasting. *Expert Syst. Appl.* **41**, 4235–4244 (2014).
62. L. Nguyen, H. W. Kinnucan, Effects of income and population growth on fish price and welfare. *Aquac. Econ. Manag.* **22**, 244–263 (2018).
63. J. Guillen, F. Maynou, Characterisation of fish species based on ex-vessel prices and its management implications: An application to the Spanish Mediterranean. *Fish. Res.* **167**, 22–29 (2015).
64. C. Costello, D. Ovando, T. Clavelle, C. K. Strauss, R. Hilborn, M. C. Melnychuk, T. A. Branch, S. D. Gaines, C. S. Szuwalski, R. B. Cabral, D. N. Rader, A. Leland, Global fishery prospects under contrasting management regimes. *Proc. Natl. Acad. Sci.* **113**, 5125–5129 (2016).
65. R. Summers, International price comparisons based upon incomplete DATA*. *Rev. Income Wealth* **19**, 1–16 (1973).
66. W. Swartz, R. Sumaila, R. Watson, Global ex-vessel fish price database revisited: A new approach for estimating 'Missing' Prices. *Environ. Econ.* **56**, 467–480 (2013).
67. A. Heston, R. Summers, B. Aten, Penn World Table Version 7.1, Center for International Comparisons of Production, Income and Prices at the University of Pennsylvania, Philadelphia (CHASS Data Centre, 2012).
68. C. C. C. Wabnitz, L. Teh, W. W. L. Cheung, in *Dynamic Integrated Marine Climate, Biodiversity, Fisheries, Aquaculture and Seafood Market Model (DIVERSE)*, W. W. L. Cheung, M. A. Oyinlola, Eds. (Institute for the Oceans and Fisheries, The University of British Columbia, 2019).
69. M. B. Schaefer, Some considerations of population dynamics and economics in relation to the management of the commercial marine fisheries. *J. Fish. Board Can.* **14**, 669–681 (1957).
70. V. W. Y. Lam, U. R. Sumaila, A. Dyck, D. Pauly, R. Watson, Construction and first applications of a global cost of fishing database. *ICES J. Mar. Sci.* **68**, 1996–2004 (2011).
71. U. R. Sumaila, D. Pauly, "Catching more bait: A bottom-up re-estimation of global fisheries subsidies" (Fisheries Centre, University of British Columbia, 2006).
72. U. R. Sumaila, V. Lam, F. Le Manach, W. Swartz, D. Pauly, Global fisheries subsidies: An updated estimate. *Mar. Policy* **69**, 189–193 (2016).
73. B. C. O'Neill, E. Kriegler, K. Riahi, K. L. Ebi, S. Hallegatte, T. R. Carter, R. Mathur, D. P. van Vuuren, A new scenario framework for climate change research: The concept of shared socioeconomic pathways. *Clim. Chang.* **122**, 387–400 (2014).
74. K. Riahi, D. P. van Vuuren, E. Kriegler, J. Edmonds, B. C. O'Neill, S. Fujimori, N. Bauer, K. Calvin, R. Dellink, O. Fricko, W. Lutz, A. Popp, J. C. Cuaresma, S. KC, M. Leimbach, L. Jiang, T. Kram, S. Rao, J. Emmerling, K. Ebi, T. Hasegawa, P. Havlik, F. Humpenöder, L. A. Da Silva, S. Smith, E. Stehfest, V. Bosetti, J. Eom, D. Gernaat, T. Masui, J. Rogelj, J. Strefler, L. Drouet, V. Krey, G. Luderer, M. Harmsen, K. Takahashi, L. Baumstark, J. C. Doelman, M. Kainuma, Z. Klimont, G. Marangoni, H. Lotze-Campen, M. Obersteiner, A. Tabeau, M. Tavoni, The shared socioeconomic pathways and their energy, land use, and greenhouse gas emissions implications: An overview. *Glob. Environ. Chang.* **42**, 153–168 (2017).
75. B. Jones, B. C. O'Neill, Spatially explicit global population scenarios consistent with the Shared Socioeconomic Pathways. *Environ. Res. Lett.* **11**, 84003 (2016).
76. D. Zeller, M. L. D. Palomares, A. Tavakolie, M. Ang, D. Belhabib, W. W. L. Cheung, V. W. Y. Lam, E. Sy, G. Tsui, K. Zylich, D. Pauly, Still catching attention: Sea Around Us reconstructed global catch data, their spatial expression and public accessibility. *Mar. Policy* **70**, 145–152 (2016).
77. W. G. Harrison, G. F. Cota, Primary production in polar waters: Relation to nutrient availability. *Polar Res.* **10**, 87–104 (1991).
78. M. I. O'Connor, J. F. Bruno, S. D. Gaines, B. S. Halpern, S. E. Lester, B. P. Kinlan, J. M. Weiss, Temperature control of larval dispersal and the implications for marine ecology, evolution, and conservation. *Proc. Natl. Acad. Sci.* **104**, 1266–1271 (2007).
79. J. A. Fernandes, W. W. L. Cheung, S. Jennings, Modelling the effects of climate change on the distribution and production of marine fishes: Accounting for trophic interactions in a dynamic bioclimate envelope model. *Glob. Chang. Biol.* **19**, 2596–2607 (2013).
80. N. A. Rayner, P. Brohan, D. E. Parker, C. K. Folland, J. J. Kennedy, M. Vanicek, T. Ansell, S. F. B. Tett, Improved analyses of changes and uncertainties in sea surface temperature measured in situ since the mid-nineteenth century: The HadSST2 Dataset. *J. Clim.* **19**, 446–469 (2006).
81. S. Schlunegger, K. B. Rodgers, J. L. Sarmiento, T. Ilyina, J. P. Dunne, Y. Takano, J. R. Christian, M. C. Long, T. L. Frölicher, R. Slater, F. Lehner, Time of emergence and large

ensemble intercomparison for ocean biogeochemical trends. *Glob. Biogeochem. Cycles* **34**, e2019GB006453 (2020).

82. W. W. L. Cheung, R. D. Brodeur, T. A. Okey, D. Pauly, Projecting future changes in distributions of pelagic fish species of Northeast Pacific shelf seas. *Prog. Oceanogr.* **130**, 19–31 (2015).

Acknowledgments: We acknowledge the suggestions and comments from D. Pauly.

Funding: W.W.L.C. thanks the Hans Sigrist Foundation and the Oeschger Centre for Climate Change Research for financial support for his residence at the University of Bern. W.W.L.C. also acknowledges funding support from the Natural Sciences and Engineering Research Council of Canada (Discovery Grant), the Social Sciences and Humanities Research Council of Canada through the OceanCanada Partnership, The Nippon Foundation–The University of British Columbia Nereus Program, and the Killam Research Fellowship. T.L.F. thanks the Swiss National Science Foundation (PP00P2_170687 and PP00P2_198897) and the European Union's Horizon 2020 research and innovation programme under grant agreement no. 820989 (project COMFORT: Our common future ocean in the Earth system—quantifying coupled cycles of carbon, oxygen, and nutrients for determining and achieving safe operating spaces with respect to tipping points) for financial support and the CSCS Swiss National Supercomputing Centre for computing resources. W.W.L.C. thanks Compute Canada for the provision of advanced research computing resources. C.C.C.W. acknowledges funding support

from The Nippon Foundation–The University of British Columbia Nereus Program, the Walton Family Foundation (grant 2018-1371), the David and Lucile Packard Foundation (grant 2019-68336), and the Gordon and Betty Moore Foundation (grant GBMF5668.02). Funding provided to C.C.C.W. under these grants has been critical to support her time. **Author contributions:** W.W.L.C. and T.L.F. conceived and designed the study. W.W.L.C. did the main analysis and wrote the first draft of the manuscript. All authors contributed to the acquisition, analysis, and interpretation of data and the writing of the manuscript. **Competing interests:** The authors declare that they have no competing interests. **Data and materials availability:** All data needed to evaluate the conclusion in the paper are present in the paper and/or the Supplementary Materials. The data that support the findings of this study are available from Dryad (<https://datadryad.org/stash/share/FHsU9YO3qYRBbQB-AzkzFYWY3Y2sFFQjN0y9ufoGtyA>).

Submitted 15 February 2021

Accepted 9 August 2021

Published 1 October 2021

10.1126/sciadv.abh0895

Citation: W. W. L. Cheung, T. L. Frölicher, V. W. Y. Lam, M. A. Oyinlola, G. Reygondeau, U. R. Sumaila, T. C. Tai, L. C. L. Teh, C. C. C. Wabnitz, Marine high temperature extremes amplify the impacts of climate change on fish and fisheries. *Sci. Adv.* **7**, eabh0895 (2021).

Marine high temperature extremes amplify the impacts of climate change on fish and fisheries

William W. L. Cheung Thomas L. Frölicher Vicky W. Y. Lam Muhammed A. Oyinlola Gabriel Reygondeau U. Rashid Sumaila Travis C. Tai Lydia C. L. Teh Colette C. C. Wabnitz

Sci. Adv., 7 (40), eabh0895. • DOI: 10.1126/sciadv.abh0895

View the article online

<https://www.science.org/doi/10.1126/sciadv.abh0895>

Permissions

<https://www.science.org/help/reprints-and-permissions>

Use of think article is subject to the [Terms of service](#)

Science Advances (ISSN) is published by the American Association for the Advancement of Science. 1200 New York Avenue NW, Washington, DC 20005. The title *Science Advances* is a registered trademark of AAAS. Copyright © 2021 The Authors, some rights reserved; exclusive licensee American Association for the Advancement of Science. No claim to original U.S. Government Works. Distributed under a Creative Commons Attribution NonCommercial License 4.0 (CC BY-NC).